



Cite this: *Lab Chip*, 2019, 19, 3344

## Wireless colorimetric readout to enable resource-limited point-of-care†

Suzanne Smith, <sup>a</sup> Adelaide Oberholzer,<sup>a</sup> Jan G. Korvink, <sup>b</sup>  
 Dario Mager <sup>\*b</sup> and Kevin Land <sup>a</sup>

A scalable, generic wireless colour detector for point-of-care diagnostics in resource-limited settings is presented. The challenges faced in these settings have limited the effectiveness of point-of-care diagnostics. By combining the growing fields of paper-based diagnostics and printed electronics with Southern African clinic perspectives, a mass-producible, low-cost, paper-based solution for result readout and communication was developed. Printed radio frequency identification devices with sensing capabilities were manufactured, targeting colour detection from lateral flow test strip devices and other typical paper-based rapid test formats. The results were compared to those obtained from a commercial lateral flow test strip reader and image analysis using ImageJ, and demonstrate suitability for delivering automated readout and communication of results. The wireless colour detector is compatible with different test strip form factors, providing a modular solution and reducing the need for training. The solution is low cost and maintenance free, and thus fitting for resource-limited settings. A scalable version of the solution has been developed, making use of standard manufacturing processes for printing and packaging industries, initially using sheet-to-sheet formats, but with the goal of being scalable to roll-to-roll processes. This would enable the possibility of local manufacture, and mass distribution of the devices to those resource-limited areas where they are most needed, and where they will have the greatest impact on point-of-care testing.

Received 11th June 2019,  
 Accepted 30th August 2019

DOI: 10.1039/c9lc00552h

rsc.li/loc

## 1. Introduction

The presented work addresses the need for low-cost, automated solutions for readout and capture of point-of-care (POC) diagnostic results that conform to the requirements of resource-limited clinics, specifically in Southern Africa. Currently insurmountable constraints in these settings, such as cost, infrastructure and trained staff, have limited the effective implementation of diagnostics at the POC, with the primary challenges lying in the accurate result readout and communication of results among clinics, hospitals and laboratories.<sup>1–3</sup> Additional problems highlighted by extensive literature regarding POC testing in South Africa<sup>4–11</sup> include the increased workload that POC devices introduce to clinics, as user training is required and test times may be lengthy. The maintenance of equipment and supply of consumables are also challenges to contend with,<sup>10</sup> along with data connectivity.<sup>11</sup> This work aims to address these challenges

through the development of a low-cost, automated readout solution that is tailored to resource-limited settings and their limitations.

The unique challenges faced in these settings have also been highlighted by the ASSURED criteria (Affordable, Sensitive, Specific, User friendly, Rapid and Robust, Equipment-free and Deliverable to end-users) as set out by the World Health Organization,<sup>12</sup> and more recently, the modified REASSURED criteria<sup>13</sup> to include newer technologies. Paper-based diagnostics, which include typical lateral flow test (LFT) formats such as pregnancy tests, as well as paper-based microfluidics,<sup>14–18</sup> are well suited to meeting many of the REASSURED aspects. This is evident from the success of simple yes/no rapid tests, where over 100 million malaria and HIV LFTs are performed every year per disease, with the majority carried out in resource-limited areas.<sup>19</sup> However, there are large discrepancies in test performance between clinics and laboratories, largely due to user error.<sup>20</sup> As an example, for HIV tests carried out at twelve primary health care facilities in South Africa, more than 4% of tests resulted in false diagnoses,<sup>20</sup> leading to knock on effects in terms of spread of disease and stigma. The goal of this work is to provide a solution that automates result readout and capturing of results from these simple test formats to reduce these errors and align with important aspects of the REASSURED criteria.

<sup>a</sup> Materials Science and Manufacturing, Council for Scientific and Industrial Research (CSIR), Pretoria, South Africa

<sup>b</sup> Institute for Microstructure Technology, Karlsruhe Institute of Technology (KIT), Karlsruhe, Germany. E-mail: dario.mager@kit.edu

† Electronic supplementary information (ESI) available. See DOI: 10.1039/c9lc00552h



External instrumentation solutions have been explored to provide automated readout from paper-based tests, including smart phones for colour readout,<sup>21,22</sup> portable potentiostats<sup>23</sup> and custom-developed add-on instrumentation.<sup>24–26</sup> Colour detection is most frequently employed for result readout from paper-based tests,<sup>27</sup> but many of these solutions remain costly and require training and maintenance. The remote location of many of the clinics makes maintenance difficult, resulting in large numbers of faulty equipment.

As an example, a module failure rate of more than 40% was reported for early results obtained from Gene Xpert MTB/RIF® systems implemented in nine countries.<sup>28,29</sup> This figure includes a test failure rate of more than 10%, but the remaining failure rate is attributed to irregular power supplies, dust build up, overheating, and a lack of staff quality control.<sup>28,29</sup> These instrumentation challenges are compounded by issues such as theft in South Africa, where mobile phone solutions are not desirable.

Printed functionality offers a potential solution, following a low-cost, maintenance-free approach to automation of paper-based diagnostics.<sup>30–32</sup> Advances in the field of printed functionality have enabled fully printed or hybrid printed components, multilayer devices, circuits and communication modules to be developed.<sup>33–38</sup> Furthermore, paper production, printing and packaging are long-standing, scalable and widely available processes, even in the targeted areas such as Southern Africa and India.

Initial case studies for the deployment of paper-based diagnostics into clinic settings have been explored,<sup>39</sup> but the implementation of feasible integrated paper-based solutions from a Southern African clinic perspective is currently lacking. Through assessment of current South African clinic workflow restrictions and needs, devices for readout and capturing of results can be developed accordingly. The presented work combines paper-based diagnostics and printed functionality with the requirements of South African clinics to provide a unique solution for POC diagnostics that is low cost, low maintenance, with the goal of being manufactured locally and supplied sustainably.

## 2. Methods

### 2.1 Clinical

Five clinics or community health centres were visited within Tshwane districts 1, 5, 6 and 7 in South Africa, and interviews were conducted with five professional nurses with an average work experience of 26 years each. The clinic patient numbers per month ranged from 4000 to 24 000. The interview questionnaires were designed to assess the greatest challenges faced, as well as current workflows for patient and result tracking and documentation. Ethics approval was obtained from the CSIR Ethics Committee once the project was registered with the National Department of Health in South Africa and permission forms were completed and signed for each district and establishment visited. All research was performed in

accordance with the relevant guidelines and regulations. Informed consent was obtained from all participants.

Site visits to clinics in South Africa, along with interviews conducted, enabled current workflows of clinics and their limitations to be summarized (Fig. 1a). Manual processes for result readout, capture and communication, along with sample and result tracking, constitute the current workflow bottlenecks, confirming published work regarding clinic workflows and challenges in South Africa and reaffirming the need to develop low-cost, automated methods for result readout and capture.

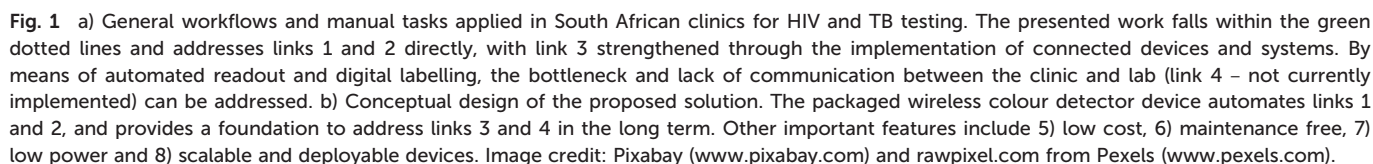
Further points that emerged from this study included adversity to the use of mobile phones as tools in clinic settings, with theft being a primary concern. Moreover, harsh environmental conditions and a lack of skilled technicians result in equipment that is not maintained. Consequently, faulty equipment is used for diagnosis, or equipment is simply unused or discarded.

### 2.2 Proposed solution

To tackle these challenges, a low-cost, maintenance-free packaged solution was developed, enabling automated readout and wireless communication of results (Fig. 1b). Wireless communication limits user handling errors and contamination. Radio frequency identification (RFID) was chosen as the method of wireless communication, as it can be utilized for device tracking, identification and management, and enables a passive, low-cost part to be separate from an external “black box” module that contains added processing capabilities (Fig. 1b). Ultra-high frequency (UHF) RFID lends itself to ease of printing of antennas with simple designs, and guaranteed read ranges of centimetres to metres. UHF RFID solutions with sensing capabilities have emerged as promising tools.<sup>40</sup> The SL900A (AMS, Austria) provides an attractive integrated circuit (IC) solution, with a variety of on-board sensing capabilities, thereby negating the need for additional complex circuitry. Previous printed component development on which this work is based includes the printing of RFID tags with the SL900A onto different flexible substrates,<sup>41</sup> as well as example applications of SL900A RFID tags, including fluidic sensing and temperature readout.<sup>42,43</sup>

The passive low-cost reader device is sufficiently low in cost as it can be disposed of after several tens to hundreds of uses, without the need for maintenance. The device does not require on-board power; instead, it can harness power from the RF field when within the range of the reader. This is illustrated in the ESI† provided. A battery was utilized in this work to enable consistent and repeatable measurements to be made, but will not be included in the final device. The device may be either passive (without a battery) or active (with a battery), with the former reducing the cost considerably and increasing the long-term reliability. In cases where batteries are required for powering additional on-board functional components, printed batteries could be utilized.<sup>44</sup>





For the LFTs, a 525 nm green LED (LTST-C190TGKT, Lite-On, Taiwan) was used to maximize the absorbance of real-world LFTs that utilize colloidal gold to enhance the perceived complementary red colour for optimal detection of the colloidal gold concentration. The LFTs developed in house make use of 40 nm colloidal gold with a peak absorbance between 520 and 525 nm, typically around 523 nm (CG-010, DCN Diagnostics, USA), closely aligned with the peak wavelength of the LED. For the pH tests, a white LED

A reusable printed RFID-based tag for colour detection and result communication was developed using hybrid printed



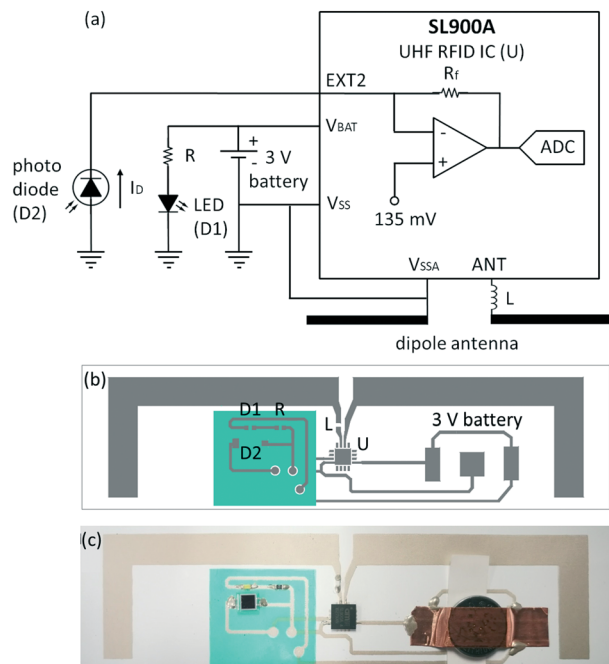


**Fig. 2** Wireless colour detector tag design illustrating a) schematic of sensing RFID tag;  $R_f = 185\text{ k}\Omega$ ,  $R = 120\text{ }\Omega$ ,  $L = 39\text{ nH}$ . Image credit: photodiode, LED and inductor by Arthur Shlain, resistor by Michael Senkow, from the Noun Project. b) Printed design of tag. c) Assembled printed wireless colour detector tag. Tag dimensions =  $110\text{ mm} \times 30\text{ mm}$ .

(VLMW1300-GS08, Vishay Intertechnologies, USA) was used to provide a broader detection spectrum, and could also be utilized with paper-based tests that implement a variety of colours.

**2.3.2 Printing and assembly.** Manual screen printing was carried out using a ZelPrint LT300 stencil printer (LPKF Laser and Electronics, Germany), modified to house screens manufactured by Chemosol (Pty) Ltd. (Johannesburg, South Africa). A synthetic mesh with 71 threads per cm (71/180-55 PW, SEFAR® PET 1500) was used with a conductive silver screen printable ink (AG-800, Applied Ink Solutions, USA), cured in an oven at  $90\text{ }^\circ\text{C}$  for 15 minutes, and a UV-curable dielectric ink (Loctite EDAG 452SS E&C, Henkel, USA), cured at a wavelength of  $365\text{ nm}$  using a handheld UV lamp (3UV-38, UVP, UK) for 4 hours. The designs were printed onto a white vinyl adhesive film (800 Premium Cast, Avery Dennison, USA). A two-component silver epoxy conductive adhesive (186-3616 RS Pro Silver, RS Components), curable at room temperature in 24 hours was used to mount and secure the various SMD components. Copper adhesive tape (3M Copper Foil Tape 1126, Digikey, USA) was used to secure the coin cell battery.

**2.3.3 Testing.** The wireless colour detector readout was performed using the RFID reader development kit (AS3993-QF\_DK\_R Fermi reader, AMS, Austria), which is recommended for use with the SL900A and includes a monopole antenna connected to a reader module with a USB interface to connect to the user interface software, where the

sensor values can be read out directly. The power transmitted by the reader was  $22\text{ dBm}$ , with reader sensitivity set to the default value of  $-68\text{ dBm}$ . The reader settings were selected with Korea (917–920 MHz) as the region, as this covers the standard South African frequency range for RFID (915–919 MHz). The packaged wireless colour detector devices were placed below the reader at a close proximity to ensure that the device could be detected reliably, and instantaneous sensor readout of EXT2 was performed through the user interface.

The analogue-to-digital converter (ADC) sensor value can be retrieved directly through the AS3993 reader user interface software. Modifications were made to the standard C++ user interface software for the reader development kit, to perform calculations directly on the sensor readout and enable the sensor value to be stored to a text file. Thresholding methods can be used to determine whether a result is positive or negative, or to establish the concentration or pH value, and to either provide instantaneous feedback to the user regarding the test results through a user interface or store the result for retrieval or analysis at a later stage.

The LED and photodiode combination were first tested, with light intensity measurements compared to a commercial light meter (Table S1†). Spacing of  $2\text{ mm}$  was used between the LFT and LED/photodiode to enable the largest dynamic range for the photodiode sensor readout values (Fig. S3, Table S2†).

Six wireless colour detector device tags were printed and assembled on transparency and adhesive vinyl substrates to illustrate the functionality on low-cost, flexible substrates that could easily be incorporated into packaged devices. The tags were assembled in a poly(methyl methacrylate) (PMMA) enclosure to facilitate a repeatable test set-up, and placed in a sealed cardboard box to provide a controlled lighting environment surrounding the PMMA device (Fig. S2†). Testing was carried out in inconsistent lighting conditions within different laboratory and office spaces to assess the effectiveness of the cardboard box in sealing tag devices from external light.

The results indicated a successful semi-quantitative distinction between different model LFT devices (Fig. S6†). Based on these results, a paper-based, scalable packaged design was developed and tested using both the model and real world LFTs to assess the functionality of the wireless colour detector devices.

## 2.4 Packaging and integration

A scalable packaging design was realized using inputs from a local packaging company (Merrypak, South Africa). The device provides a modular solution, adaptable to various paper-based test formats.

The matchbox-style design (Fig. 1b and S7†) was printed in a single-sheet format (one sheet for the inner tray and one sheet for the outer sleeve) on white glossy cardboard (King Pearl Design 210 GMS, Stationery and Print, South Africa) and manually cut out, creased, folded and glued for the



prototypes used in this work. Graphics were printed on the outer sleeve to provide product information, user instructions and a QR code for electronic information.

The printed and assembled RFID tags (Fig. 2c) were mounted on the boxes prior to assembling the packaged devices. The inserts for the tray component of the box were made from lightweight 10 mm thick cardboard packaging (Kimmoboard, Kimmo (Pty) Ltd., South Africa) and were cut to size using a jigsaw. The cut-outs were covered with white vinyl as a protective layer, with an additional 1 mm thick vinyl-covered cardboard layer mounted on top and a custom cut-out for the specific test format used, such as cassette or test strip. A flexible vinyl ribbon with an arrow was attached under the insert to assist with pulling the tray out to insert a test. The dimensions of the final packaged wireless colour detector devices are 140 mm × 45 mm × 20 mm.

The packaged wireless colour detector devices were tested with the 12 model LFT devices housed in plastic cassettes, with results that were comparable to the initial tests using model LFT devices in the repeatable PMMA enclosure set-up (Fig. S9 and S10†).

For automated production, existing commercial printing and packaging methods including die cutting are feasible, in which print designs are provided for the front and reverse in large sheet formats. Once printed, automated cutting, creasing and gluing are carried out to produce the cardboard box packaging.

## 2.5 Real world rapid tests

Commercial rapid tests (Clicks ovulation test, Clicks Pharmacies, South Africa) were used as initial yes/no real-world tests (Fig. S11†). These are qualitative test strips housed in plastic cassettes that are used to predict when there is a surge in luteinizing hormone (LH) levels in urine. A negative female urine sample was collected and immediately tested using the dropper supplied with the rapid test kit to introduce the sample to the cassette and run the test to produce a control line. Ethics approval was obtained from the CSIR Ethics Committee. All research was performed in accordance with the relevant guidelines and regulations. Informed consent was obtained from the human subject participating in the experiment.

LFTs developed and manufactured at the CSIR, South Africa, for the detection of *E. coli* in contaminated water samples were utilized as semi-quantitative real-world tests (Fig. S12†). Dilutions were made from cultured bacteria using a phosphate buffer to obtain different bacteria concentrations or colony-forming units per ml (cfu ml<sup>-1</sup>) for testing purposes. The samples tested in this study included the phosphate buffer (negative control), tap water, 3 × 10<sup>6</sup> cfu ml<sup>-1</sup>, 3 × 10<sup>7</sup> cfu ml<sup>-1</sup>, 3 × 10<sup>8</sup> cfu ml<sup>-1</sup> and a black test line created using a permanent marker on an unused LFTs, as an additional calibration sample. The hook effect, in which excess antibodies or antigens in the test cause false-negatives or false low results,<sup>48</sup> causes the 3 × 10<sup>7</sup> cfu ml<sup>-1</sup> samples to

produce a darker test line than the higher 3 × 10<sup>8</sup> cfu ml<sup>-1</sup> concentrations.

To investigate different test formats, home-use pH test strips (Clicks alkaline/acid pH test strips, Clicks Pharmacies, South Africa) were utilized. These test kits are supplied with a colour chart to determine pH values in the range of 5.5 to 9.5 (Fig. S13b†). The pH 6, 8 and 9 solutions were made from a pH 7 neutral standard, using a pH meter (pHscan30L Pocket pH, Bante Instruments, China) to confirm the pH values.

**2.5.1 Usability.** An initial usability study (Fig. S13b and S15†) was formulated to assess the packaged wireless colour detector devices, as user friendliness is an important consideration and an ASSURED requirement. Six participants with an average age of 34.5 (±13.8) were asked to assess the devices through a questionnaire that was formulated, and to perform a user test using the pH test strips to assess the functionality of the reader devices in real-world conditions. One of the participants was a retired nurse, while one had no previous experience with medical devices or rapid tests. The participants were provided with a user guide and were requested to carry out a practical test with the pH test strips. Participants were asked to read out the results both manually, using a colour chart, and using the packaged reader device for an automated readout. Once the test was completed, the participants completed a questionnaire to assess the usability of the packaged reader devices and note areas of improvement in future developments. Ethics approval was obtained from the CSIR Ethics Committee. All research was performed in accordance with the relevant guidelines and regulations. Informed consent was obtained from all participants. Details of the usability study can be found in the ESI† and Fig. S14.

## 3. Results

### 3.1 Real-world rapid test analysis

**3.1.1 Yes/no lateral flow tests.** Initial real-world tests were carried out using commercial over-the-counter rapid tests (Fig. 3a). For each cassette, the wireless colour detector device recorded sensor readouts for the dry or unused test, negative test line and positive control line. Five low-cost reader devices using tags printed on white adhesive vinyl were tested, with three different rapid tests analysed per reader. The results were normalized to the dry unused test, and enabled clear distinctions to be drawn between the negative and positive test results (Fig. 3b).

Larger variations are present in the readout for positive results, and are primarily caused by the positioning or alignment of the control line relative to the detection mechanism inside the box. However, clear distinctions can be made between the negative and positive results, with no readout errors present across all tests and reader devices for a threshold value of 0.89. Threshold values can be optimized through more extensive testing, and individual thresholds can be determined for each device.



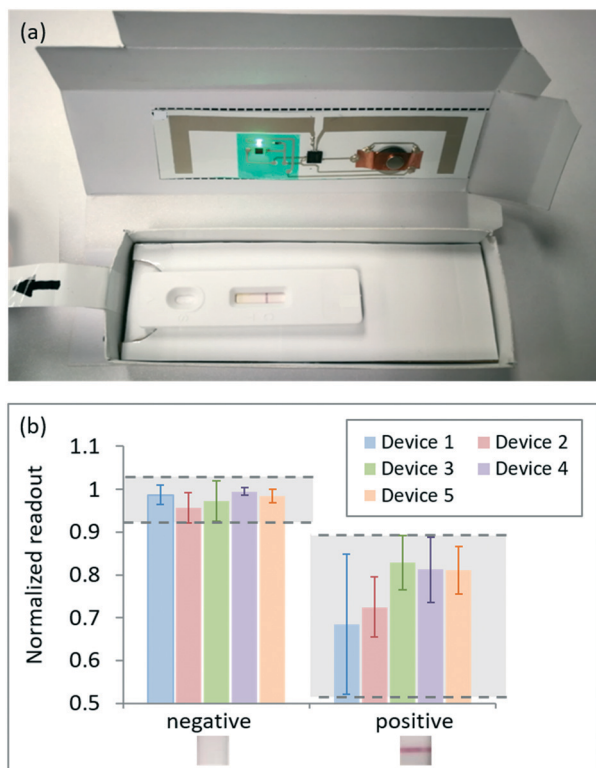


**Fig. 3** a) Inside view of box with insert for housing LFT cassette positioned inside tray and with printed tag mounted inside sleeve of box. b) Average normalized results for negative and positive test results for five tags, along with test results for each individual tag, each tested with three rapid test cassettes. Shaded areas indicate the range of measurements across the packaged wireless colour detector devices, highlighting distinct readout ranges for positive and negative test results.

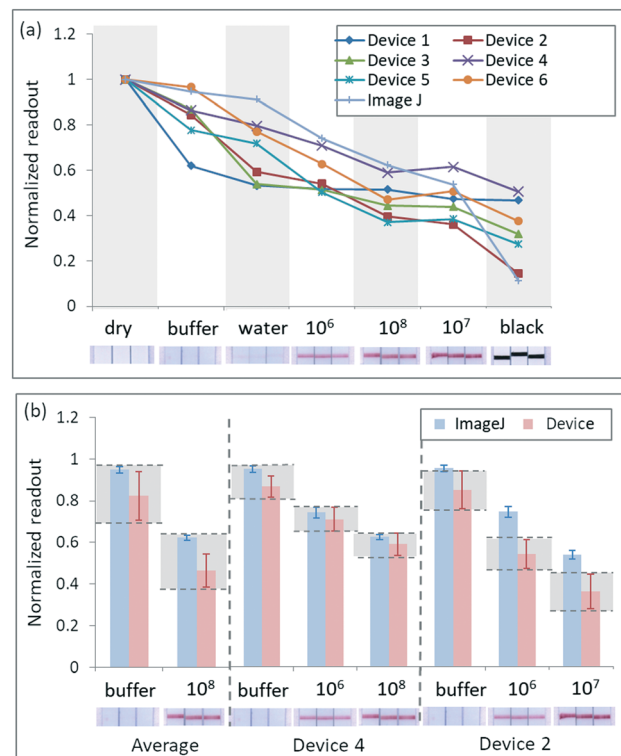


**Fig. 4** a) Normalized results for 6 reader devices compared to normalized ImageJ results (average over 3 LFT readings) for different bacteria concentrations (cfu ml<sup>-1</sup>). b) Normalized results for average over 6 reader devices compared to normalized ImageJ results to show distinction between negative (buffer) test strips and concentrations of 10<sup>8</sup> cfu ml<sup>-1</sup>, along with device with smallest variations (device 4) and largest variations (device 2) compared to ImageJ results for 3 different *E. coli* concentrations. Shaded areas indicate measurement ranges across packaged wireless colour detector devices, highlighting distinct readout ranges for different bacteria concentrations.

**3.1.2 Semi-quantitative lateral flow tests.** LFTs for the detection of *E. coli* contamination in water were assessed to determine the semi-quantitative readout capabilities of the low-cost readers. Six low-cost reader devices were tested, with three LFTs assessed for each sample concentration (Fig. 4). The results were normalized to the dry, unused tests for each reader device. The LFTs were scanned (Fig. S12b†) and ImageJ analysis was performed (Fig. S8†) as a baseline with which to compare the results obtained using the low-cost reader devices.

The 10<sup>7</sup> cfu ml<sup>-1</sup> concentration is visually darker than the 10<sup>8</sup> cfu ml<sup>-1</sup> concentration as a result of the hook effect. The results are presented from the lowest signal (buffer) to the highest (10<sup>7</sup> cfu ml<sup>-1</sup>) for ease of analysis and trend comparisons. Across all reader devices, a clear distinction can be made between a negative and positive test result (Fig. 4b). Thresholding can again be used to determine whether a test result is negative or positive. With a threshold setting of 0.65, an 11.11% error is obtained (two false positives using device 1) across all devices and repeats tested.

Two low-cost reader devices were compared to the ImageJ results to demonstrate that semi-quantitative analysis is possible (Fig. 4b). Device 4 had the smallest variations across measurements (±6%) and similar trends and values to the

ImageJ reference results, while device 2 had the largest variations across measurements (±15%) and values that were further from the ImageJ reference values. The results indicate that semi-quantitative analysis is possible for discriminating between different concentrations of *E. coli*.

Distinct ranges are defined for device 4 for each concentration, with no errors. The values also fall within the range of the ImageJ reference values for each concentration. Uncertainty exists in the discrimination between 10<sup>8</sup> cfu ml<sup>-1</sup> and the darkest 10<sup>7</sup> cfu ml<sup>-1</sup> concentrations, but for discrimination between more faint signals, the results indicate a clear distinction between concentrations. For device 2, the results do not fall within the same range of values as the ImageJ results, but distinct ranges are defined for each concentration, enabling discrimination between different concentrations. Device 2 is less sensitive than device 4, as a clear distinction can only be made between 10<sup>6</sup> cfu ml<sup>-1</sup> and 10<sup>7</sup> cfu ml<sup>-1</sup> (darkest colour) effectively, with some uncertainty in the discrimination between 10<sup>6</sup> cfu ml<sup>-1</sup> and 10<sup>8</sup> cfu ml<sup>-1</sup> as well as between 10<sup>8</sup> cfu ml<sup>-1</sup> and 10<sup>7</sup> cfu ml<sup>-1</sup>.

**3.1.3 Different test formats.** Commercial pH test strips were used to test a different test format with the packaged





wireless colour detector devices, and to perform initial usability studies. Five low-cost reader devices were tested, each with six tests per pH value. In each case, pH test strips from two different test kits were used (three from one, three from the other) to incorporate variations in the test strip colours across test kits. A new strip was tested each time. The test results were normalized to the dry, unused test strip (yellow colour), which also assists in accounting for variations in colour from one test kit to another, where significant visual differences can be noted across test kits. pH solutions of 6, 7, 8 and 9 were tested. ImageJ analysis was performed following a similar approach to the ImageJ analysis carried out for the semi-quantitative LFTs and used as a baseline with which to compare the results obtained using the low-cost reader devices. Although the average packaged reader device results do not fall in the same range as the greyscale values determined for each pH concentration, distinct ranges were obtained without errors for pH 6, 7 and 8, with uncertainty in the discrimination between pH 8 and 9 (Fig. 5c). Reliable readout using the packaged reader devices depends on a large enough difference in greyscale values between the different pH test strips, with a difference of between 15 and 20 greyscale units being the minimum for reliable discrimination, corresponding to normalized greyscale differences of approximately 0.1 and 0.15 for the tests conducted.

**3.1.4 Usability.** Based on the results of Fig. 5b, pH solutions of 6, 7 and 9 were utilized for the usability study to ensure that the devices could determine the pH value effectively. Calibration of each tag device was performed using thresholds defined for each device and for each pH value in the usability study (Table S4 and Fig. S14†). This approach can be optimized through more extensive testing to ensure that minimal errors are produced.

Participants performed pH test strip analysis using both a manual colour chart readout and the automated low-cost reader solution. A total of eight tests were carried out by the six participants. In all cases, participants required only one attempt to obtain a result from the device (effectiveness = 1). The average time for users to perform the task (efficiency) was 35 seconds ( $\pm 20$  seconds) for the manual readout and 5 seconds ( $\pm 3$  seconds) for the automated readout. The total time required to complete the task for both the manual and automated readouts, including gaining an operational understanding of the device *via* the user guide and wetting a test strip in a selected sample, was 2 minutes 20 seconds ( $\pm 30$  seconds). Among the tests carried out, two manual colour chart readout results were correctly interpreted, while six automated results using the packaged reader devices were correctly read out. The results show promise for device functionality under real testing conditions with little user training. According to the questionnaires completed by the participants, the average usability score using the system usability scale (SUS) was 84.17 ( $\pm 6.23$ ) out of 100 and the overall satisfaction score using the after scenario questionnaire (ASQ) was 6.39 ( $\pm 0.39$ ) out of 7. Generally, the users were satisfied with the usability of the reader devices, with the main challenges focussed on the box

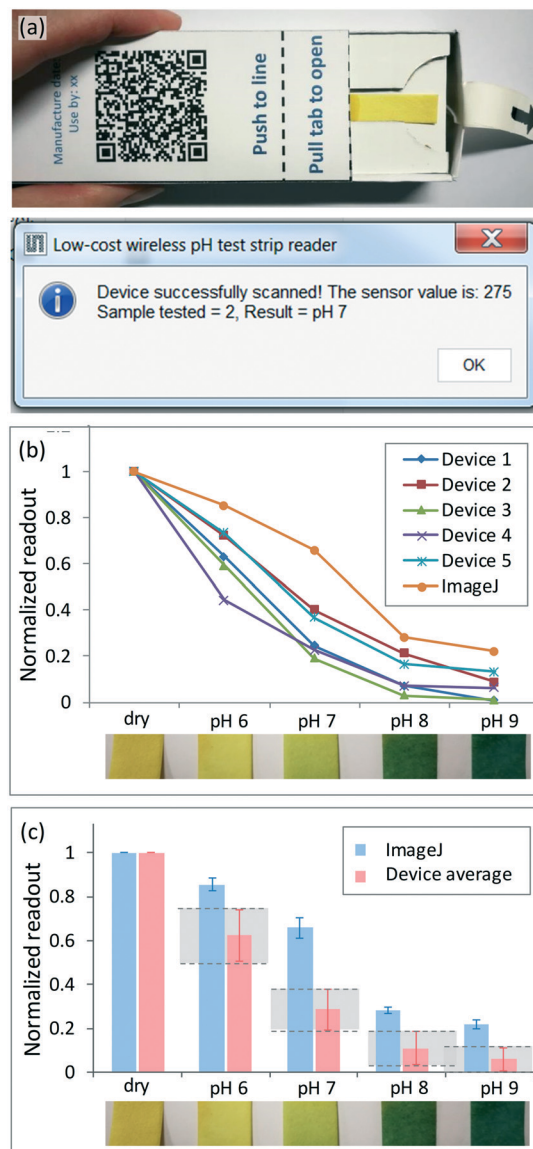


Fig. 5 a) pH analysis showing pH test strip inserted into packaged wireless colour detector device and automated wireless result readout through user interface. b) Normalized results for 5 packaged wireless colour detector devices, with each pH value tested 6 times, and compared to normalized ImageJ analysis results. c) Normalized average results indicating distinct ranges obtained for each pH value and compared to normalized ImageJ analysis results.

sliding mechanism, the positioning of the test strip in the insert and the positioning or alignment of the tray inside the sleeve for correct alignment. Issues regarding the mechanical components will likely be addressed by mass production, with prototypes currently being manually assembled, while other aesthetic and functional inputs will be considered in the next iteration of prototypes.

### 3.2 Wireless connectivity and data capturing

Extensive read range measurements for tags assembled on different substrates have previously been reported.<sup>41</sup> Read



range measurements for tag devices inside the PMMA enclosure, as well as inside the PMMA enclosure and the cardboard box sealed from external light, were also carried out (Table S3†). Building on this, the maximum read ranges at which the photodiode sensor values could still be read out wirelessly through the RFID reader user interface were recorded. Read range measurements were performed on 10 tag devices assembled into the cardboard boxes, and with LFTs housed in cassettes inside the cardboard boxes. The read ranges were recorded with the battery connected to emulate real-world testing conditions, as the LED is currently driven using the battery. Initial tests were performed to demonstrate that the LED can successfully be powered using the RF field generated when the device is within the range of the reader (Fig. S16†). However, to ensure reliable test conditions and eliminate potential fluctuations in LED intensity, a battery was used to drive the LED in this work. The read ranges varied between 35 and 180 mm, with an average of 97.5 mm ( $\pm 51.6$  mm). As discussed in previous work,<sup>41</sup> these would be adequate read ranges for use in clinic environments, as envisaged for these devices.

Automated data capturing occurs when the packaged reader device is scanned using the RFID reader. Direct feedback is provided *via* a graphical user interface and the sensor values are stored in a text file. The standard C++ user interface software for the AS3993 reader development kit was modified, with threshold calculations implemented for the different sensor values read out (*e.g.* Table S4†). This enabled additional feedback to be provided *via* the user interface, and the results to be written to a file for data storage and traceability. The data acquisition process is error-free, as data is stored directly onto a computer. Further data management can be implemented using standards for medical data handling, such as Health Level Seven (HL7) international electronic healthcare information standards.<sup>49</sup>

### 3.3 Costing

The cost of a low-cost packaged reader device using the current manual manufacturing and assembly techniques can be estimated at EUR 21. For medium scale automated manufacture, the cost per device drops to approximately EUR 13, while for high volume automated production, a cost of EUR 4 can be projected. An initial cost of less than EUR 562 per RFID reader system mounted and secured in a clinic has been costed by a local RFID company, and would be lower for scaled up production of the reader devices. The price of a commercial benchtop lateral flow test reader is typically in the region of EUR 1875, and indicates that the solution proposed in this work would be approximately a third of the cost of solutions that are currently utilized.

## 4. Discussion

The colour detection results obtained for real-world tests in inconsistent testing environments and lighting conditions enabled result capture and communication through RFID,

and were comparable to the image analysis results obtained using ImageJ. Moreover, the initial usability tests suggest that the current format can already be utilized for screening and semi-quantitative test readout requirements (Fig. 3–5). The packaged wireless colour detector allows for various paper-based test formats to be analysed, providing a modular solution that contributes to the low-cost, accessible nature of the approach.

Variations were observed in the measured colour intensity results for a single reader device, and are a result of the currently manual assembly methods, in which the positioning of the SMD components affects the results. Furthermore, the battery voltage affects the intensity of each LED and thus the measured sensor value. Calibration methods have been implemented to account for these inter-device inconsistencies through normalization of the measured sensor values to the dry or unused test strip, and could be extended to incorporate additional reference colours for calibration, yielding more accurate and quantitative colour detection capabilities. Automated matching of the reference measurements captured from an individual device to the unique device identification number (specific to the RFID IC) when a device is scanned could improve the readout accuracy.

A green LED was used for the LFT devices, as it is well suited to the detection of colloidal gold, while white LEDs were implemented for the pH test strips to provide a broader detection spectrum, and could be extended to other paper-based tests that utilize various colours. Different photodetectors and spacings between light sources and detectors were explored, with the SFH 2430 providing a large dynamic range for the sensor measurements obtained, without adjusting the parameters in the SL900A ADC.

Printability of the devices onto low-cost substrates – specifically for packaged solutions – has been explored,<sup>46</sup> and offers the potential to align with current printing and packaging processes. Initial feasibility and cost analyses have been carried out to assess the system scalability utilizing local production capabilities, which is desirable from both cost and accessibility perspectives. Sheet-to-sheet printing of functional inks, such as silver and dielectric, are possible using screens with multiple designs, and larger-scale printing of functional inks by local companies is currently being explored. Once devices are printed, individual devices need to be cut and creased, either manually or by using standard packaging production lines. Thereafter, assembly of all required electronic components is performed; currently manually, but with the option of using small-scale pick and place equipment and low-temperature solder paste, which is currently being explored in conjunction with a local university. In the long term, it may be possible to incorporate large-scale pick and place production lines using roll-to-roll formats, in which case assembly could be carried out prior to cutting and creasing. Packaging for the printed tags has been investigated with a local packaging company for prototyping, and a packaging scale-up would be feasible and cost-effective in the future.





The printability of the various SMD components can be explored further towards the long-term goal of a fully integrated printed solution. This has been investigated in house for printed inductors (Fig. S17†), as well as printed primary batteries for use with the SL900A printed tags.<sup>43</sup> Current research and development on printed light sources, such as organic LEDs (OLEDs)<sup>50</sup> and light-emitting electrochemical cells (LECs),<sup>51</sup> which have successfully been implemented on paper-based substrates, could be utilized in future, as well as printed photodetectors.<sup>52</sup> A recent example showcasing printed photodiode arrays<sup>53</sup> could be applied for multiplexed tests and more complex readouts in future. The in-house development of an inkjet printed RFID tag on photo paper using the die format of the SL900A chip has successfully been demonstrated,<sup>54</sup> and has also been initially explored for screen printed tags (Fig. S17†), indicating promise for a more flexible, low-cost and readily disposable solution for this key RFID tag component.

Although the current performance of the low-cost packaged reader devices requires further optimization, a solution that addresses the most important challenges in South African resource-limited clinic settings – including cost, maintenance, as well as bottlenecks and errors in result readout and capture – has been demonstrated. Additional unique challenges such as theft are also taken into account. As the development of the low-cost packaged reader devices progresses, incorporating feedback from users performing field tests in resource-limited settings will be imperative to ensure that effective, usable solutions are developed.

## 5. Conclusions

The Ideal Clinics programme<sup>55</sup> has been formulated by experts in the field as a guideline for future South African clinics, and the present work addresses important aspects including infrastructure and communication, applicable to administration and digital health system support. As part of this programme, and from a clinic perspective, this work can initially assist with patient and result identification and tracking information, thereby alleviating the data management requirements and burden on already constrained resources. Future work may include RFID labelling of individual tests, so that the tests and reader devices can be linked to further assist with traceability. An integrated, modular system approach, as presented in this work, would enable resource-limited settings to improve diagnosis and healthcare infrastructure in the long-term.

Successful implementation of the packaged reader and similar devices will depend on the ability to scale manufacture to produce high volumes of devices, along with the supply chain infrastructure to ensure deployment to remote settings. In addition to scalability and deployment considerations, disposability will form an important part of the development process from the early stages for large scale feasible, sustainable and environmentally friendly POC solutions to be realized.

## Author contributions

S. S. led the experimental work and manuscript write-up, and designed the devices. S. S. and A. O. manufactured, assembled and tested the devices. D. M., J. G. K. and K. L. assisted with the experimental design and analysis of results. All authors contributed to and reviewed the manuscript.

## Conflicts of interest

There are no conflicts to declare.

## Acknowledgements

The authors gratefully acknowledge the Council for Scientific and Industrial Research (CSIR), Pretoria, South Africa, and the Karlsruhe Institute of Technology (KIT), Germany, for funding this work. Specifically, the authors acknowledge support by the Deutsche Forschungsgemeinschaft and the KIT-Publication Fund of the Karlsruhe Institute of Technology. The authors thank Thabang Noge and Alma Truys from the CSIR for their assistance with the LFT device manufacturing and testing, as well as for providing bacterial and pH dilutions. Phophi Madzivhandila is thanked for assistance with the printing, assembly and testing of tag devices. Special thanks are extended to the participants who contributed to the usability studies, and to Hildegard Prigge for assistance with the illustrations in Fig. 1.

## References

- 1 N. Engel, M. Davids, N. Blankvoort, N. P. Pai, K. Dheda and M. Pai, *Trop. Med. Int. Health*, 2015, **20**, 493–500.
- 2 T. P. Mashamba-Thompson, N. A. Jama, B. Sartorius, P. K. Drain and R. M. Thompson, *Diagnostics*, 2017, **7**, 3.
- 3 B. Cheng, B. Cunningham, D. I. Boeras, P. Mafaune, R. Simbi and R. W. Peeling, *Afr. J. Lab. Med.*, 2016, **5**, 535.
- 4 P. K. Drain and C. Rousseau, *Curr. Opin. HIV AIDS*, 2017, **12**, 175–181.
- 5 L. Oldach, *Lab Culture ASLM Magazine*, 2015, vol. 13, pp. 7–17.
- 6 L. E. Scott, *SAMJ*, 2013, **103**, 883–884.
- 7 J. O. T. Anstey Watkins, J. Goudge, F. X. Gómez-Olivé and F. Griffiths, *Soc. Sci. Med.*, 2018, **198**, 139–147.
- 8 W. Stevens, N. Gous, N. Ford and L. E. Scott, *BMC Med.*, 2014, **12**, 173.
- 9 K. Blattner, G. Nixon, C. Jaye and S. Dovey, *Afr. J. Prim. Health Care Fam. Med.*, 2010, **2**, 54–60.
- 10 N. M. Gous, L. E. Scott, J. Potgieter, L. Ntabeni, I. Sanne and W. S. Stevens, *J. Acquired Immune Defic. Syndr.*, 2016, **71**, e34–e43.
- 11 W. D. Meyer, *PathCare Pathology Forum – Point of Care*, 2013, vol. 4, pp. 24–25.
- 12 D. Mabey, R. W. Peeling, A. Ustianowski and M. D. Perkins, *Nat. Rev. Microbiol.*, 2004, **2**, 231–240.
- 13 K. J. Land, D. I. Boeras, X. S. Chen, A. R. Ramsay and R. W. Peeling, *Nat. Microbiol.*, 2019, **4**, 46–54.



- 14 K. Yamada, H. Shibata, K. Suzuki and D. Citterio, *Lab Chip*, 2017, 17, 1206–1249.
- 15 A. Nilghaz, L. Guan, W. Tan and W. Shen, *ACS Sens.*, 2016, 1, 1382–1393.
- 16 A. W. Martinez, S. T. Phillips, M. J. Butte and G. M. Whitesides, *Angew. Chem., Int. Ed.*, 2007, 46, 1318–1320.
- 17 A. W. Martinez, S. T. Phillips, G. M. Whitesides and E. Carrilho, *Anal. Chem.*, 2010, 82, 3–10.
- 18 A. K. Yetisen, M. S. Akram and C. R. Lowe, *Lab Chip*, 2013, 13, 2210–2251.
- 19 K. J. Land, S. Smith and R. W. Peeling, in *Paper-based Diagnostics*, ed. K. Land, Springer, Cham, Switzerland, 2019, pp. 1–21.
- 20 D. Moodley, P. Moodley, T. Ndabandaba and T. Esterhuizen, *SAMJ*, 2008, 98, 707–711.
- 21 A. W. Martinez, S. T. Phillips, E. Carrilho, S. W. Thomas, H. Sindi and G. M. Whitesides, *Anal. Chem.*, 2008, 80, 3699–3707.
- 22 J. Hu, S. Wang, L. Wang, F. Li, B. Pingguan-Murphy, T. J. Lu and F. Xu, *Biosens. Bioelectron.*, 2014, 54, 585–597.
- 23 J. L. Delaney, E. H. Doeven, A. J. Harsant and C. F. Hogan, *Anal. Chim. Acta*, 2013, 803, 123–127.
- 24 P. Bezuidenhout, S. Smith and T.-H. Joubert, *Appl. Sci.*, 2018, 8, 968.
- 25 H. Liu and R. M. Crooks, *Anal. Chem.*, 2012, 84, 2528–2532.
- 26 C. Zhao, M. M. Thuo and X. Liu, *Sci. Technol. Adv. Mater.*, 2013, 14, 54402.
- 27 G. G. Morbioli, T. Mazzu-Nascimento, A. M. Stockton and E. Carrilho, *Anal. Chim. Acta*, 2017, 970, 1–22.
- 28 I. Pathmanathan, A. Date, W. L. Coggin, J. Nkengasong, A. S. Piatek and H. Alexander, *Afr. J. Lab. Med.*, 2017, 6, a460.
- 29 J. Creswell, A. J. Codlin, E. Andre, M. A. Micek, A. Bedru, E. J. Carter, R.-P. Yadav, A. Mosneaga, B. Rai, S. Banu, M. Brouwer, L. Blok, S. Sahu and L. Ditiu, *BMC Infect. Dis.*, 2014, 14, 2.
- 30 T. Ahmadraji, L. Gonzalez-Macia, T. Ritvonen, A. Willert, S. Ylimaula, D. Donaghy, S. Tuurala, M. Suhonen, D. Smart, A. Morrin, V. Efremov, R. R. Baumann, M. Raja, A. Kemppainen and A. J. Killard, *Anal. Chem.*, 2017, 89, 7447–7454.
- 31 V. Beni, D. Nilsson, P. Arven, P. Norberg, G. Gustafsson and A. P. F. Turner, *ECS J. Solid State Sci. Technol.*, 2015, 4, S3001–S3005.
- 32 S. Smith, J. G. Korvink, D. Mager and K. Land, *RSC Adv.*, 2018, 8, 34012–34034.
- 33 J. S. Chang, A. F. Facchetti and R. Reuss, *IEEE J. Emerg. Sel. Top. Circuits Syst.*, 2017, 7, 7–26.
- 34 Y. Wang, H. Guo, J. Chen, E. Sowade, Y. Wang, K. Liang, K. Marcus, R. R. Baumann and Z. Feng, *ACS Appl. Mater. Interfaces*, 2016, 8, 26112–26118.
- 35 X. Zhang, T. Ge and J. S. Chang, *Org. Electron.*, 2015, 26, 371–379.
- 36 S. Khan, L. Lorenzelli and R. S. Dahiya, *IEEE Sens. J.*, 2015, 15, 3164–3185.
- 37 F. Alimenti, C. Mariotti, V. Palazzi, M. Virili, G. Orecchini, P. Mezzanotte and L. Roselli, *Journal of Low Power Electronics and Applications*, 2015, 5, 151–164.
- 38 U. Kavčič, M. Maček and T. Muck, *J. Imaging Sci. Technol.*, 2015, 59, 505041–505048.
- 39 A. A. Kumar, J. W. Hennek, B. S. Smith, S. Kumar, P. Beattie, S. Jain, J. P. Rolland, T. P. Stossel, C. Chunda-Liyoka and G. M. Whitesides, *Angew. Chem., Int. Ed.*, 2015, 54, 5836–5853.
- 40 J. Zhang, G. Tian, A. Marindra, A. Sunny and A. Zhao, *Sensors*, 2017, 17, 265.
- 41 S. Smith, A. Oberholzer, K. Land, J. G. Korvink and D. Mager, *Flexible Printed Electron.*, 2018, 3, 025002.
- 42 S. Smith, P. H. Bezuidenhout, K. Land, J. G. Korvink and D. Mager, *SPIE Proc. Fourth Conference on Sensors, MEMS, and Electro-Optic Systems*, 2017, 10036, p. 100360J.
- 43 S. Smith, A. Oberholzer, P. Madzivhandila, K. Land, J. G. Korvink and D. Mager, *Proc. SPIE Fifth Conference on Sensors, MEMS, and Electro-Optic Systems*, 2019, 11043, p. 110430I.
- 44 A. M. Gaikwad, A. C. Arias and D. A. Steingart, *Energy Technol.*, 2015, 3, 305–328.
- 45 S. Smith, K. Land, J. G. Korvink and D. Mager, presented in part at 21st International Conference on Miniaturized Systems for Chemistry and Life Sciences (MicroTAS 2017), Savannah, Georgia, USA, October, 2017.
- 46 S. Zhou, W. Ling and Z. Peng, *Int. J. Adv. Manuf. Technol.*, 2007, 33, 837–844.
- 47 C. Occhiuzzi, C. Vallese, S. Amendola, S. Manzari and G. Marrocco, *Procedia Comput. Sci.*, 2014, 32, 190–197.
- 48 J. Schiettecatte, E. Anckaert and J. Smitz, in *Advances in Immunoassay Technology*, ed. N. H. L. Chiu, InTech, available from: <http://www.intechopen.com/books/advances-in-immunoassay-technology/interference-in-immunoassays>, 2012.
- 49 Health Level Seven International, <http://www.hl7.org/>, (accessed June 2018).
- 50 S. Purandare, E. F. Gomez and A. J. Steckl, *Nanotechnology*, 2014, 25, 094012.
- 51 A. Asadpoordarvish, A. Sandström, C. Larsen, R. Bollström, M. Toivakka, R. Österbacka and L. Edman, *Adv. Funct. Mater.*, 2015, 25, 3238–3245.
- 52 G. Pace, A. Grimoldi and M. Sampietro, *Semicond. Sci. Technol.*, 2015, 30, 104006.
- 53 I. Deckman, P. B. Lechêne, A. Pierre and A. C. Arias, *Org. Electron.*, 2018, 56, 139–145.
- 54 P. Bezuidenhout, S. Smith, K. Land and T.-H. Joubert, *Electron. Lett.*, 2019, 55, 252–254.
- 55 Department of Health, Republic of South Africa, Ideal clinic definitions, components and checklists, <https://www.idealclinic.org.za/>, (accessed October 2017).

